Vol. 747: 35–48, 2024
https://doi.org/10.3354/meps14698

MARINE ECOLOGY PROGRESS SERIES
Mar Ecol Prog Ser

Published October 17

Phytoplankton size structures and their interactive effects with nutrient conditions on sinking rates in a mariculture system

Xiaofei Tian, Yufeng Ye, Yucheng Li, Lili Diao, Yihang Wang, Xiaolong Yang, Xiumei Zhang*

Fishery College, Zhejiang Ocean University, 1 Haida South Road, Changzhi Island Lincheng New Area, Zhoushan 316022, PR China

ABSTRACT: Phytoplankton sinking rates (Srs) are often considered to be the predominant method through which organic matter is delivered out of the surface euphotic zone. Although the phytoplankton size structures (PSSs) are considered to be responsible for the Srs, which are in turn regulated by nutrient levels, their interactive effects on Srs are not so well studied. To address this knowledge gap, we measured the PSSs and their Srs, along with environmental variables including nitrate, nitrite, ammonium, phosphate, temperature (*T*), salinity, and dissolved oxygen in summer and winter in a mussel farm. We found spatial variations in PSSs in both seasons. Owing to the size-selective feeding of mussels, the activity of the mussel farm may influence the spatial distribution of the phytoplankton community. The dominant PSSs were >20 and <20 µm phytoplankton in summer and winter, respectively, suggesting seasonal variations in PSS. These dominant size groups were negatively related to nitrate in summer and positively related to *T* in winter, suggesting that nitrate and *T* may have played roles in influencing the PSS. In summer, micro- and pico-sized phytoplankton strongly affected their Srs in opposite directions, which were in turn mainly regulated by nitrate, indicating that nitrate may affect the Sr indirectly via PSS. Meanwhile, a direct effect of nitrate on Sr was found in both seasons but in opposite directions, suggesting a mutual interaction between Sr and nitrate. These results imply that in a mariculture system, the drivers of phytoplankton carbon export may involve multiple factors with complicated interactive effects.

KEY WORDS: Environmental variables · Nitrate · Phytoplankton · Sinking rate · Size structure

1. INTRODUCTION

Particulate organic carbon produced by phytoplankton sinks out of the euphotic layer and is partly sequestered in the sediments, efficiently promoting the absorption of atmospheric carbon dioxide by the oceans (Falkowski et al. 1998, Boyd & Trull 2007). In general, faster-sinking phytoplankton contribute more to the vertical flux of carbon, while slower-sinking ones are more easily degraded into dissolved matter by marine bacteria and are then recycled in the water column (Silver et al. 1978, Smith et al. 1992, Alcolombri et al. 2021). Since marine phytoplankton dominate primary production across ~70% of the Earth's surface (Field et al. 1998, Mattei et al. 2021), their sinking velocity is one of the main drivers in regulating ocean carbon sequestration (Guidi et al. 2016). However, the mechanisms determining phytoplankton sinking rates (Srs) remain poorly understood.

Srs often differ among different phytoplankton size groups or even species (Takahashi & Bienfang 1983, Guo et al. 2016, Mao et al. 2023), since large phyto-

*Corresponding author: smzhang1227@163.com

plankton sink faster than smaller ones (Smayda 1970). This fact suggests that phytoplankton size structures (PSSs) may play a vital role in influencing their Srs. In general, PSS and phytoplankton distribution are closely associated with various environmental factors, such as chemical, physical, and biological variables (Naselliflores 2000, Yin et al. 2011, Tian et al. 2013). Previous studies have indicated that seasonal changes in only one of these factors may impact the community of phytoplankton to a certain extent (Cetinić et al. 2006, Jiang et al. 2014). For instance, water temperature (*T*) has been shown to be an important factor affecting PSS (Peters 1983, Reuman et al. 2014, López-Urrutia & Morán 2015), and nutrient conditions in the ocean are also considered to be a critical restricting factor for the abundance and community dynamics of phytoplankton (Smith 1982, Cetinić et al. 2006, Wang et al. 2015). PSSs are considered to be responsible for the Srs, which are in turn regulated by environmental variables including nutrients (Marañón et al. 2001, 2015, Maguer et al. 2009, Acevedo-Trejos et al. 2015, Marañón 2015, Mousing et al. 2018). Thus, an assessment of the Sr of different PSSs, under different environments with detectable nutrients, may contribute to a comprehensive understanding of the dynamics of phytoplankton export from the surface to the bottom water.

In addition, Srs could also be directly influenced by a variety of environmental factors, according to both laboratory experiment (or indoor cultivation) and field observations. The influence of these environmental parameters on phytoplankton cell sinking is likely to differ in various ways; for instance, salinity (S) can influence the cellular size (Radchenko & Il'yash 2006), *T* can change the medium density (Agawin et al. 2000, Iversen & Ploug 2013), and nutrients can affect the osmotic pressure of the cells (Gemmell et al. 2016). However, external environmental parameters usually differ in their effects on particle sinking depending on spatial–temporal variability. In addition, among nutrients, nitrogen is one of the most restricting chemicals in affecting the cellular characteristics of phytoplankton, such as cellular morphology and density, and physiological state (Bienfang et al. 1982), which are the main factors regulating phytoplankton buoyancy (van Ierland & Peperzak 1984, Waite et al. 1997, Jiang et al. 2022). Accordingly, a number of studies have found that nitrate (NO_3^-) limitation may facilitate Srs in the lab (Titman & Kilham 1976, Bienfang et al. 1982, Muggli et al. 1996). However, few studies have reported the association between nutrients and Srs *in situ*.

In this study, we sampled from a mussel farm in Gouqi Island, Zhejiang province, China, where the nutrients are seasonally variable (Zhang et al. 2008, Guan et al. 2022). Although the seasonal dynamics of species composition of phytoplankton have been demonstrated (Guan et al. 2022), their PSSs and Srs have not yet been examined. Moreover, since mussels are selective filter feeders, mussel aquaculture may be a significant driver of phytoplankton dynamics in terms of size structures (Deng 2016, Zhang et al. 2024). Thus, Gouqi Island is an excellent survey area to test the interactive effects of PSSs and environmental variables on Srs. In the present study, we measured chemical and environmental variables, PSSs, and the corresponding Srs in summer and winter. The specific objectives were to determine (1) whether PSS and Sr change spatially and seasonally, and (2) whether and how the nutrients and PSSs regulate Srs. These results will contribute to our understanding of the phytoplankton carbon export and related mechanisms in coastal areas.

2. MATERIALS AND METHODS

2.1. Study area and water sampling

PSSs and Srs were measured at 5 sites (G1, G2, G3, G4, and G5) within a mussel farm around Gouqi Island, Zhejiang province, China, on 16–17 August 2021 and 7–8 December 2022 (Fig. 1). Among the sampling sites, G1 (30° 42′ 53.66″ N, 122° 44′ 57.99″ E) and G4 (30° 44′ 01.97″ N, 122° 46′ 17.36″ E) are close to the north shore of Gouqi Island, G5 (30° 43′ 34.09″ N, 122° 45′ 01.28″ E) is in the center of the farm, and G2 (30° 43′ 48.77″ N, 122° 43′ 33.58″ E) and G3 (30° 44′ 18.29″ N, 122° 45′ 04.38″ E) are relatively far from shore and near the farm boundary. At each site, the vertical profiles of *T*, S, and dissolved oxygen (DO) were measured using a Seabird conductivity, temperature, and depth (CTD) device (SBE 9/11 plus). Afterward, based on the maximum water depth at each site (Table S1 in the Supplement at www.int-res.com/suppl/articles/m747p035_supp.pdf), water samples from the surface (0.5 m) and bottom (mean ± SD: 18.80 ± 4.75 m) layers were collected separately using a water sampler (5 l bottles) for analysis of chlorophyll *a* (chl *a*) and Sr, and then the remaining water from each layer was mixed for analysis of nutrients because of the rapid vertical exchange of nutrients that occurs between surface and bottom waters, especially in the shallow coastal ocean in this study (Qu et al. 2022).

Water samples for nutrient measurement were first filtered through acid-cleaned acetate cellulose filters

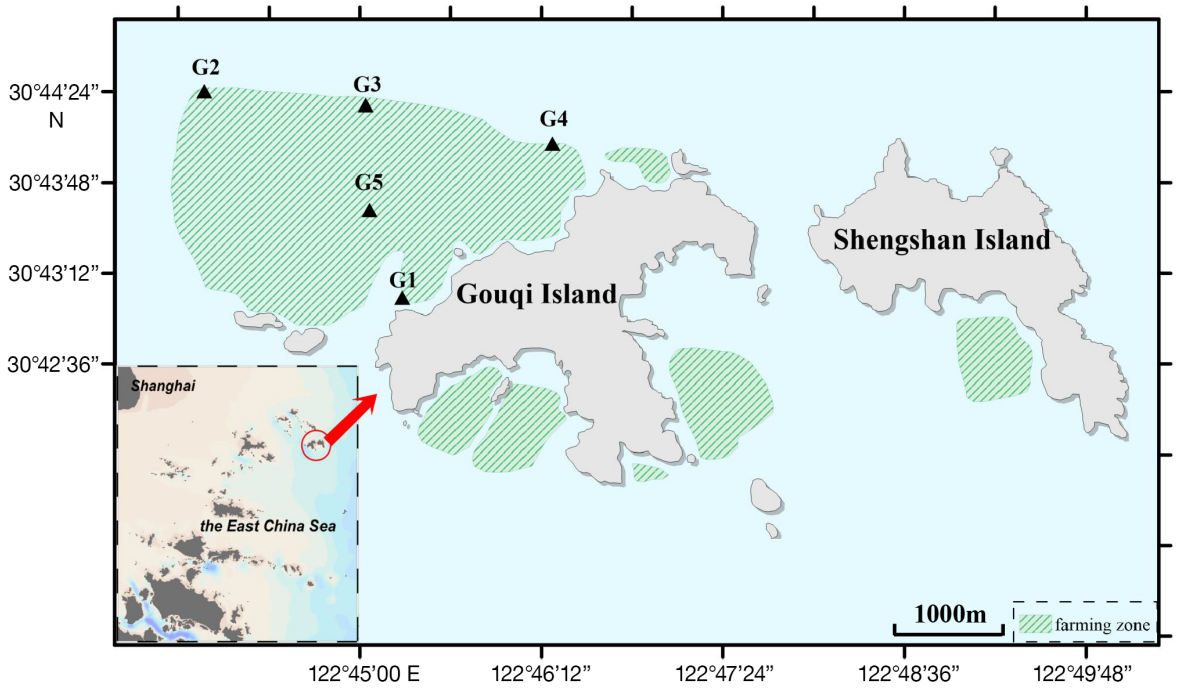

Fig. 1. Distribution of the 5 sampling sites in a mussel farm around Gouqi Island

(0.45 µm pore size). Then the filtrates were treated by adding $HgCl_2$ solution and stored in the dark at 0–4°C until use. In the laboratory, nutrients including nitrite (NO_2^-), NO_3^-, ammonium (NH_4^+), and phosphate (PO_4^{3-}) were analyzed with test kits using a spectrophotometer (HACH DR6000).

Water samples for chl *a* analysis from each of the surface and bottom layers were first poured onto filters and then maintained frozen at −20°C until analysis. Chl *a* was extracted with 90% acetone for 24 h at −20°C in the dark and measured with a spectrophotometer (HACH DR6000) (Welschmeyer 1994). To examine the proportion of different size classes of phytoplankton, we estimated the size-fractionated chl *a*. The size-fractionated filtration method for measuring chl *a* concentration in each size group involves filtering water through different filters with decreasing pore sizes. In the present study, for each site, ~1000 ml of seawater collected from each layer was filtered sequentially through a 20 µm nylon membrane, 2 and 0.2 µm polycarbonate membrane filters (47 mm; Merck Millipore) under low-vacuum pressure (<0.04 MPa). In addition, following Sieburth et al. (1978), the chl *a* concentration in each size group was defined as pico-sized, nano-sized, and micro-sized chl *a* for the size ranges of 0.2–2, 2–20, and >20 µm, respectively. Thereafter, the total chl *a* content (called 'total size-fractionated chl *a* concentration') was calculated from the sum of the 3 size groups for each sample. Thus, the contribution of each size group of chl *a* to the total chl *a* content (chl $a_{proportion}$) was defined as follows:

$$\frac{Chl\ a_{xyz}}{Pico-sized\ chl\ a_{xy} + Nano-sized\ chl\ a_{xy} + Micro-sized\ chl\ a_{xy}} \quad (1)$$

where *x*, *y*, and *z* represent the sampling site, layer, and phytoplankton size class, respectively.

Sr was examined using a SETCOL method described by Bienfang (1981) for each site at selected layers, including the surface and bottom layer in both seasons. Based on Guo et al. (2016), we modified the height and diameter of the settling column designed by Bienfang (1981). A plexiglass column with 6 cm internal diameter, 25 cm height, and 0.8 l volume was used (Fig. S1). To reduce wall effects on the particle sinking process, the column diameter was widened (Mao et al. 2023). For the analysis, the settling column was filled with a homogeneous seawater sample and capped. Then, the plexiglass column was allowed to settle undisturbed for 2–3 h (Guo et al. 2016). During incubation, the SETCOL apparatus was covered with a neutral density screen to keep the water sample in the dark. The incubation was terminated by successively draining the upper, middle, and bottom layers of the SETCOL compartments by taps through the column wall. The phytoplankton chl *a* concentration, using before and after incubation in all 3 compart-

ments, was combined to calculate Srs as follows (Mao et al. 2023):

$$\Psi = \frac{\left[V_b Chla_b - V_b\left(Chla_0 + Chla_t\right)/2\right]}{\left(V_u + V_m + V_b\right)\left(Chla_0 + Chla_t\right)/2} \times \left(\frac{L}{t}\right) \quad (2)$$

where ψ represents the Sr; V_b, V_m, and V_u represent the volume of the bottom, middle, and upper part of the column, respectively (Fig. S1); $Chla_0$ and $Chla_t$ represent the total chl *a* concentration at the beginning and end of the experiment, respectively; $Chla_b$ represents the total chl *a* concentration in the settling zone at the end of the experiment; L represents the column length; and t represents the settling interval. For each site, 3 replicate settling columns were filled with collected seawater from each sampling layer.

2.2. Statistical analysis

The Sr data and the concentrations of pico-, nano-, and micro-sized chl *a* were log transformed to stabilize the variance. Shapiro-Wilk and Levine's tests were then used to determine normality and homogeneity, respectively. After confirming that the transformed data met these assumptions, the effects of season (summer and winter), site (G1, G2, G3, G4, and G5), layer (surface and bottom), and their interactions on these data were statistically tested using a 3-way ANOVA. The 'lsmean()' function in the 'lsmean' package in R was used for post-hoc interaction analysis. Significant effects were determined at $p < 0.05$, and the α level was adjusted by a Bonferroni correction for multiple comparisons with interaction terms.

To clarify the effect of environmental factors, including nutrient concentrations of NO_2^-, NO_3^-, NH_4^+, and PO_4^{3-}, and water depth, DO, *T*, and S on the concentrations of pico-, nano-, and micro-sized chl *a* in each season, we conducted a redundancy analysis (RDA). The 'rdacca.hp.()' function in the 'rdacca.hp.' package in R was performed to evaluate the individual importance of all environmental factors on the variation in PSS composition (Lai et al. 2022). Then we examined the relationship between the proportion of each size-fractionated chl *a* group to the total size-fractionated chl *a* concentration and Sr in each season using a generalized linear model (GLM). After that, to examine the contributions of nutrient concentrations including NO_2^-, NO_3^-, NH_4^+, and PO_4^{3-}, and water depth, *T*, and S to Srs in each season, we conducted a GLM with model selection procedures. The models, composed of single variables, were performed to identify the most important variable. We selected the best-fitting model using Akaike's information criterion (AIC). We estimated the difference in AIC value (D_i) between the best fit and other models. If D_i for model i was <2, the model was treated equally as the minimally adequate model (Burnham & Anderson 2003). The conventional coefficient of determination (r^2) was used as a percentage of variation to explain the Sr. All statistical tests were performed in R v3.6.1 (R Core Team 2019).

3. RESULTS

3.1. Hydrographic conditions

Profiles of nutrient concentrations, *T*, S, and DO are shown in Table S1. In the study area, the seasonal variations in S and concentrations of NO_3^- were relatively small. Although *T* and concentrations of NH_4^+ and NO_2^- in summer were higher than in winter, the opposite result was found for DO and concentrations of PO_4^{3-}. Among the sampling sites, G1 showed a relatively high concentration of NH_4^+ and high S, especially in summer.

3.2. Total and size-fractionated chl *a* concentrations

The total size-fractionated chl *a* concentration largely differed among sampling sites regardless of sampling layer, which was higher in summer (average: 2.35 ± 0.98 µg l^{-1}) than in winter (0.57 ± 0.17 µg l^{-1}) (Fig. 2). The 3 measured size-fractionated chl *a* concentrations also varied between these 2 seasons (Table 1). Although the concentration of pico-sized phytoplankton was higher in winter than in summer, an opposite result was found for nano- and micro-sized phytoplankton (Figs. 2 & 3). In summer, the dominant size class was micro-sized phytoplankton, whose contribution to total size-fractionated chl *a* concentration (average: 80 ± 11%) was higher than that in winter (39 ± 13%) (Figs. 2 & 3), whereas the nano-sized (24 ± 10%) and pico-sized (37 ± 9%) phytoplankton represented a higher proportion of total size-fractionated chl *a* concentration in winter than in summer (i.e. an average value of 13 ± 8 and 7 ± 9% for nano- and pico-sized chl *a*, respectively) (Figs. 2 & 3).

In addition, although no difference was found between sampling layers, all 3 size-fractionated chl *a* concentrations showed large variations among sampling sites (Table 1, Fig. 3). Significant interaction effects of season, site, and layer were found on all size-fractionated chl *a* concentrations (Table 1). To

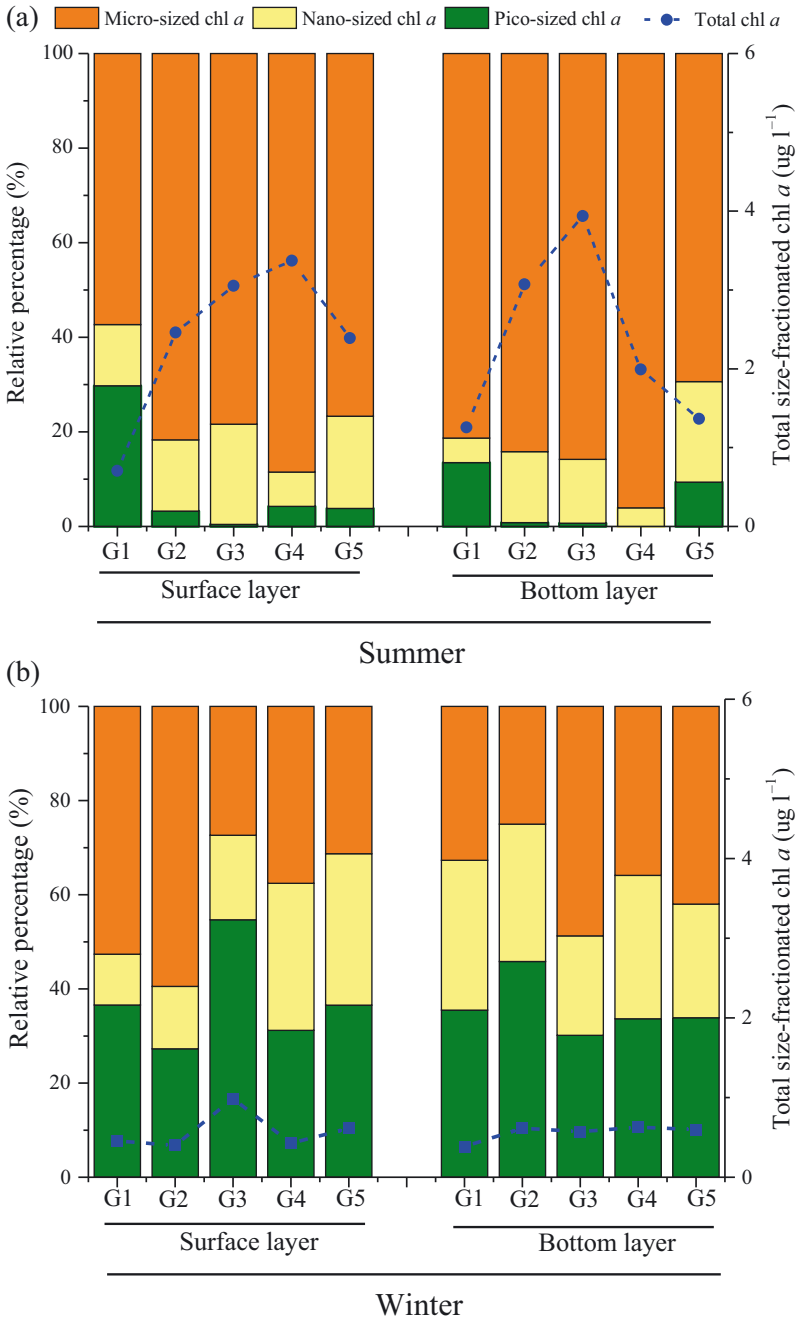

Fig. 2. Total size-fractionated chl *a* concentration and the relative proportion for each size class among sampling stations in (a) summer and (b) winter. Blue dots and lines: total size-fractionated chl *a* concentration, which was the sum of the 3 size classes

better present the multiple comparisons with the interaction terms, we examined the least-squares means for all 3 size-fractionated chl *a* concentrations at each site in each season (Table S2). We found that the concentration of pico-sized phytoplankton was relatively high at Site G1 in summer, while Site G3 showed a higher value than the other sites in winter (Fig. 3a,b). For both nano- and micro-sized phytoplankton, Site G3 represented a relatively high value than Site G1 in summer, while a similar level was found for all sites in winter (Fig. 3).

3.3. Sinking rates

Measured Srs based on the changes in chl *a* concentrations in SETCOL are presented in Fig. 3. The Srs in summer, ranging from 0.02 to 0.41 m h^{-1} (0.23 ± 0.10 m h^{-1}), were significantly higher than in winter, ranging from 0.08 to 0.35 m h^{-1} (0.20 ± 0.08 m h^{-1}) (Table 1). Although the Srs did not differ between sampling layers, they differed significantly among sites (Table 1, Fig. 4). In addition, significant interaction effects of season, site, and layer on Srs were found (Table 1). As above, the least-squares means for Srs at each site in each season were also examined (Table S2). We found that in summer, the Srs at Site G1 were significantly lower than those at Sites G3 and G4. Conversely, in winter, the Srs at Sites G3 and G5 were lower than that at Sites G1 and G4 (Fig. 4).

3.4. Relation between environmental factors and PSS

The association between environmental variables and PSS was examined using RDA. The environmental factors analyzed included *T*, S, DO, and concentrations of NH_4^+, NO_2^-, NO_3^-, and PO_4^{3-}. Among them, concentrations of NO_3^- had the highest individual importance (24.58%, p = 0.001), followed by concentrations of NH_4^+ (17.13%, p = 0.002) and DO (12.53%, p = 0.01) in summer, while *T* had the highest unique importance (8.39%, p = 0.037), followed by S (4.19%, p = 0.126) and DO (2.77%, p = 0.171) in winter (Table S3, Fig. S2). In addition, Fig. 5a shows that in summer, the first axis is positively related to micro-sized phytoplankton and *T*, while being negatively related to S and the concentration of NO_3^-. The second axis is positively related to pico-

Table 1. Results of 3-way ANOVA for the effects of season (summer and winter), sampling site (G1, G2, G3, G4, and G5), layer (surface and bottom), and their interactions on phytoplankton sinking rate and concentrations of each size-fractional chl *a* (pico-, nano-, and micro-sized phytoplankton) in Gouqi Island. Statistically significant p-values ($p < 0.05$) are in **bold**

Traits	Season (Se)		Site (Si)		Layer (L)		Se × Si × L	
	F	p	*F*	p	*F*	p	*F*	p
Sinking rate (m h^{-1})	4.322	**0.044**	17.617	**<0.001**	0.017	0.896	4.84	**0.0028**
Pico-sized chl *a* concentration (μg l^{-1})	80.581	**<0.001**	2.813	**0.038**	5.211	0.058	10.911	**<0.001**
Nano-sized chl *a* concentration (μg l^{-1})	39.358	**<0.001**	11.079	**<0.001**	0.206	0.652	3.355	**0.002**
Micro-sized chl *a* concentration (μg l^{-1})	865.306	**<0.001**	31.566	**0.011**	0.009	0.924	12.743	**<0.001**

sized phytoplankton, DO, concentrations of NH_4^+, NO_2^-, and PO_4^{3-}, while being negatively related to nano-sized phytoplankton. In winter, the first axis is positively related to S and the concentration of NO_2^-, while being negatively related to pico- and micro-sized phytoplankton. On the second axis, nano-sized phytoplankton are positively related to *T* and concentrations of NH_4^+ and PO_4^{3-}, while being negatively related to DO (Fig. 5b).

3.5. Relation between PSS and Srs

To clarify the relationship between the relative proportion of each size-fractionated chl *a* concentration and Sr in each season, we conducted a GLM (Fig. 6). In summer, the Sr was not only positively related to the proportion of micro-sized chl *a* to total size-fractionated chl *a* concentration ($r = 0.438$, $p = 0.015$) (Fig. 6c), but also negatively associated with the relative proportion of pico-sized chl *a* ($r = -0.540$, $p = 0.002$) (Fig. 6a). However, the Sr was not related to the relative proportion of nano-sized chl *a* in both seasons (Fig. 6b,e). In winter, the Sr was only negatively related to the relative proportion of pico-sized chl *a* ($r = -0.444$, $p = 0.014$) (Fig. 6d).

3.6. Modeling Srs with environmental factors

A GLM was also performed to determine the contributions of environmental factors to Srs (Table 2). When various environmental factors were considered as explanatory variables, the concentration of NO_3^- in both seasons was selected as the best single-parameter model for Sr according to AIC. Indeed, most of the variations in Sr were explained by the concentration of NO_3^- in both summer (59.4%) and winter (34.5%). However, although Sr and the concentration of NO_3^- were negatively related in summer, an opposite correlation was found in winter (Fig. 7). The concentration of NH_4^+ also proved to be significantly associated with Sr but explained only 12.6 and 28.1% of the variation in summer and winter, respectively (Table 2).

4. DISCUSSION

4.1. Phytoplankton size structures

In this study, 3 size-fractionated chl *a* concentrations (0.2–2, 2–20, and >20 μm) were determined at selected layers (surface and bottom) among 5 sites in a mussel farm around Gouqi Island. Although our study includes a limited number of survey sites, their strategic placement across the farm provides valuable insights. We designated 2 sites in the near-shore area (G1 and G4), 3 at the boundary zone (G2, G3, and again G4), and one in the central region of the farm (G5). Despite being spread across different areas, the environmental variables we monitored showed minimal variation among sites within a season, indicating a degree of uniformity in the aquatic environment. The current results showed that the concentrations of each size of phytoplankton did not differ between layers, although they differed greatly among sampling sites. This finding is in agreement with a previous study indicating that the PSSs at the surface may reflect the entire water column (Shiomoto & Inoue 2020). In addition, we found seasonal variations in the measured PSSs (cf. Yang et al. 2008, Pulina et al. 2018, Shiomoto & Inoue 2020). Among 3 size structures, micro-phytoplankton accounted for a high proportion in summer (ca. 80%) and also a relatively high proportion in winter (ca. 39%). On the other hand, smaller phytoplankton (<20 μm) occupied a higher proportion in winter (ca. 61%). These results suggest that large and smaller sizes of phytoplankton accounted for the largest proportion of the primary producers in summer and winter, respectively, in the study area.

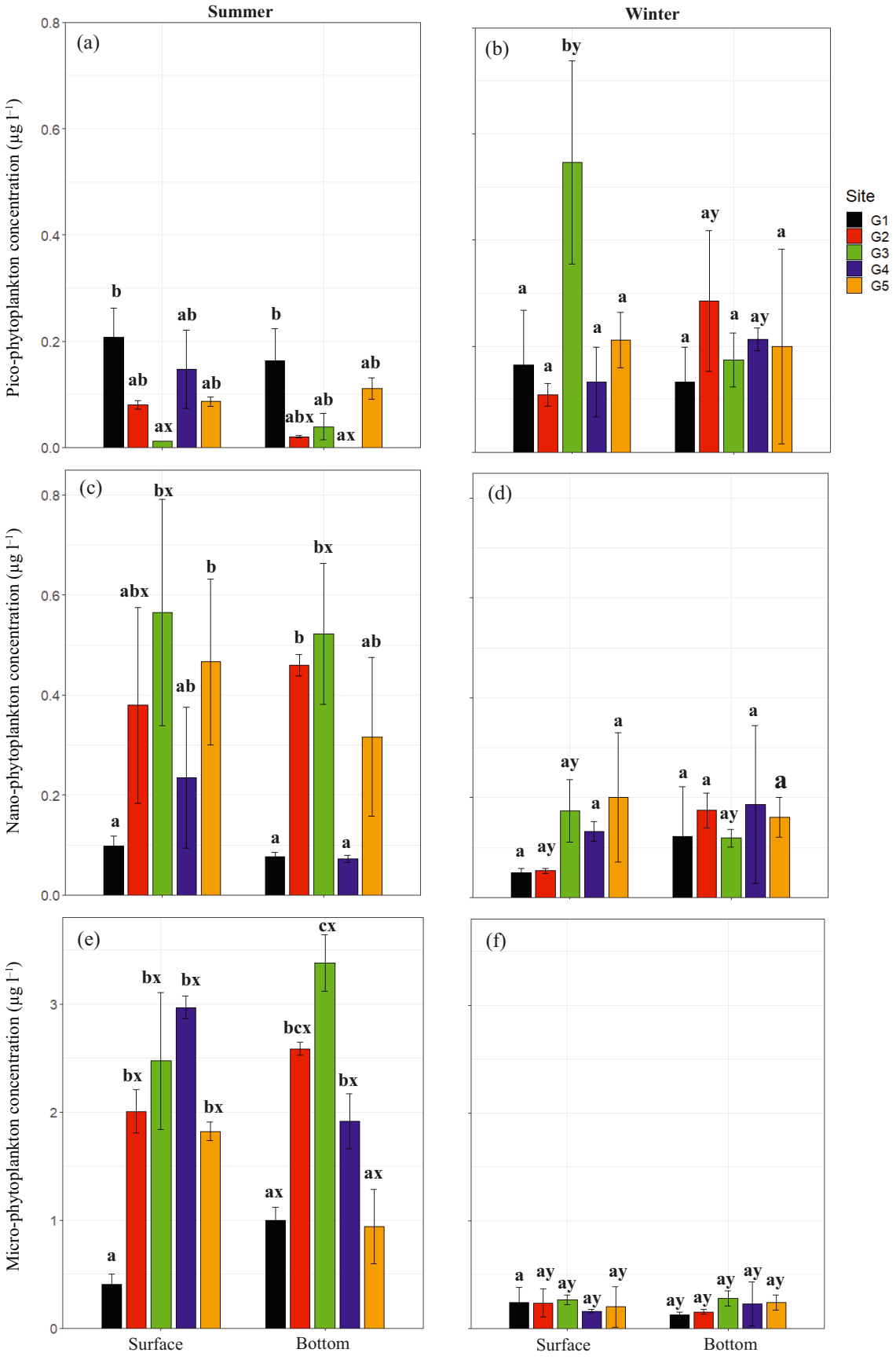

Fig. 3. Spatial variation of concentration for each size class (a,b: pico-; c,d: nano-; e,f: micro-phytoplankton) among sampling stations in (a,c,e) summer and (b,d,f) winter. Error bars: SE among the replications (n = 3). Different lowercase letters (a and b) above bars represent significant differences ($p < 0.05$) for each size class among sampling sites at each sampling layer within each season; x and y represent significant differences for each size class between seasons within each sampling site at each sampling layer. Bars with the same letter do not differ significantly

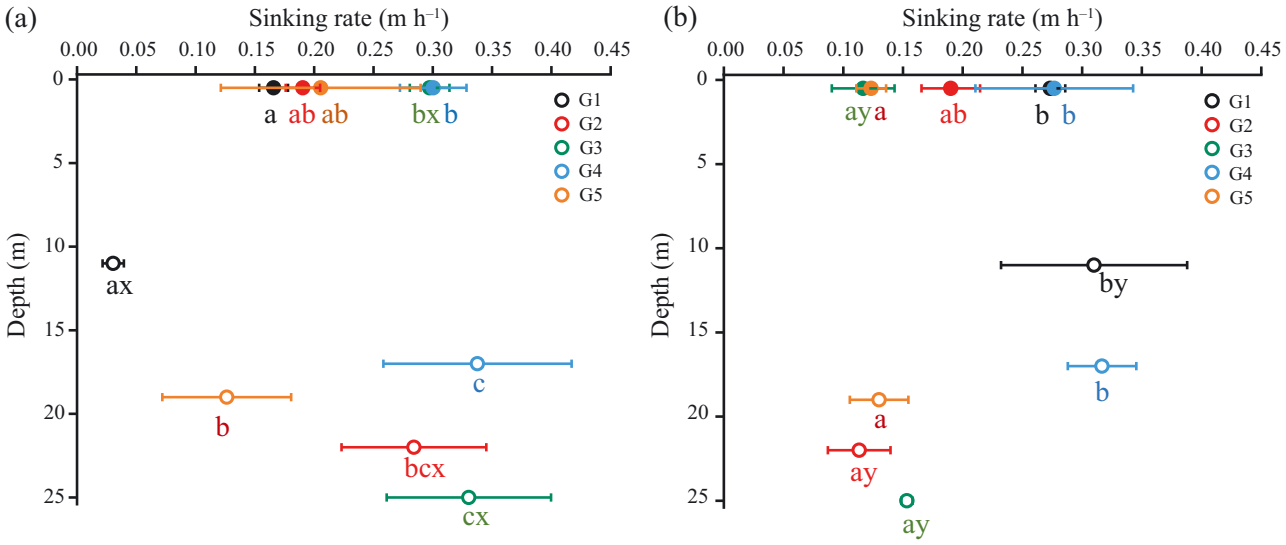

Fig. 4. Phytoplankton sinking rates measured with the SETCOL method at each sampling layer among survey stations in (a) summer and (b) winter. Error bars: SE among the replications (n = 3). Different lowercase letters (a and b) represent significant differences ($p < 0.05$) for each size class among sampling sites at each sampling layer within each season; x and y represent significant differences for each size class between seasons within each sampling site at each sampling layer. Bars with the same letter do not differ significantly

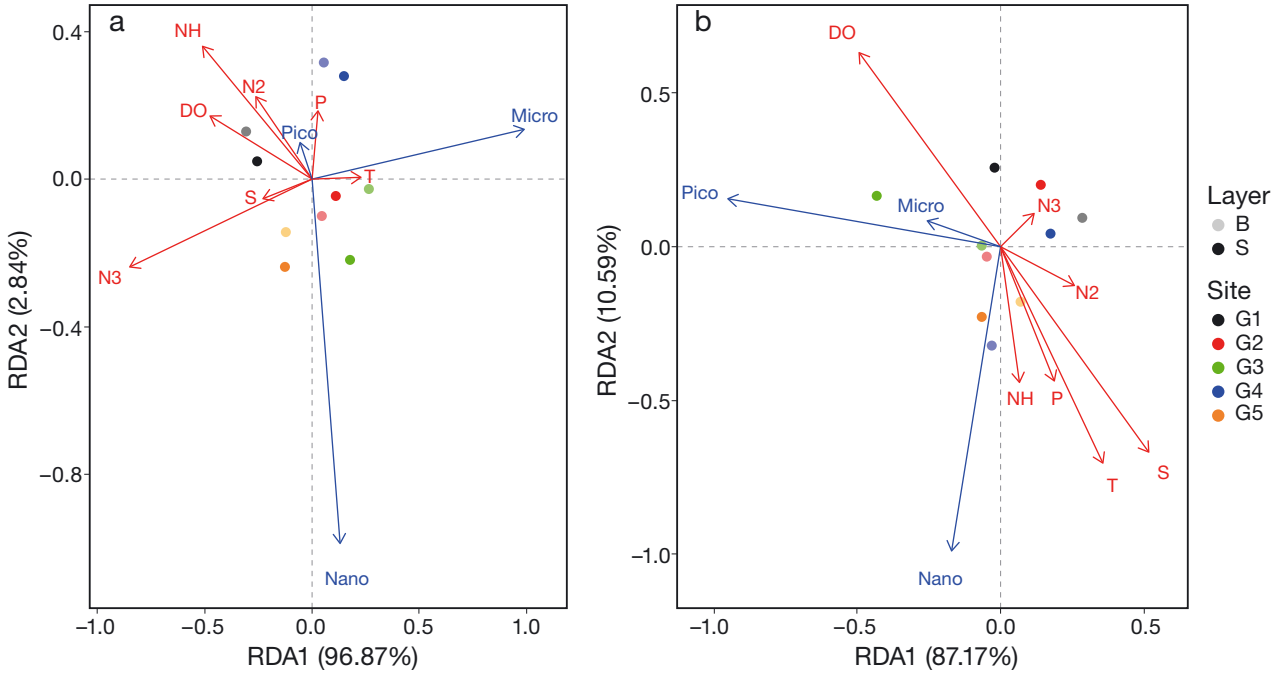

Fig. 5. Redundancy analysis (RDA) of the concentration of each phytoplankton size class with environment factors in (a) summer and (b) winter. Blue and red arrows: phytoplankton size structures and environment factors, respectively. *T*: temperature; S: salinity; DO: dissolved oxygen; N2: NO_2^-; N3: NO_3^-; NH: NH_4^+; P: PO_4^{3-}

In certain coastal regions, nanophytoplankton can constitute a significant portion of the total phytoplankton biomass and play a pivotal role in shaping the dynamics of PSSs (Kocum 2020). However, nanophytoplankton showed the lowest contribution to the total chl *a* in the mussel farm around Gouqi Island. One possibility for this phenomenon is the size-selective feeding of mussels on nano-phytoplankton. The preferred size range of phytoplankton for these mussels is 5–30 µm, with the gill cilia showing the highest retention efficiency for particles sized 10–20 µm (reaching up to 95%) and lower efficiencies for par-

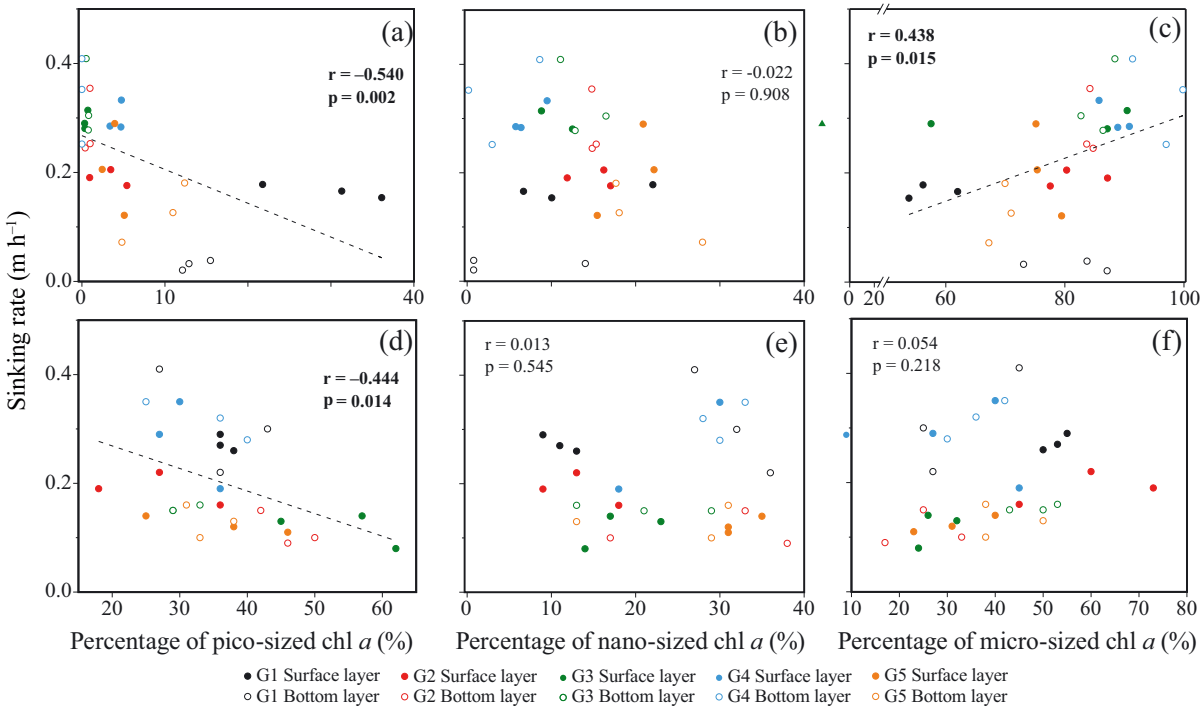

Fig. 6. Phytoplankton sinking rate fitted against the relative proportion of (a,d) pico-, (b,e) nano-, and (c,f) micro-phytoplankton in summer (a,b,c) and winter (d,e,f). The correlation coefficient (r) and significant probability (p) of the regression lines ($p < 0.05$) are shown in **bold** in the panels of statistically significant regressions

ticles smaller than 10 µm or larger than 20 µm (Li 2019). This indicates a relatively high removal rate of nano-phytoplankton by mussels in this region and, consequently, a decline in their contribution to total chl *a*. If this is the case, selective predation by intensively farmed mussels may alter the size composition of the phytoplankton community (Zhang et al. 2024).

In addition to the filter-feeding of cultured mussels, environmental factors may also play roles in impacting the PSSs. To identify the dominant factors affecting the PSS in these 2 seasons, we performed an RDA. The results showed that various environmental factors between the 2 seasons were responsible for the PSS. In winter, only *T* significantly affected the PSS and was positively associated with smaller phytoplankton (2–20 µm), suggesting that the proportion of smaller phytoplankton increased with increasing *T* in winter (Atkinson et al. 2003, Marañón et al. 2012, López-Urrutia & Morán 2015). Moreover, we found that the concentration of most nutrients was relatively low in winter. Compared to the large plankton species, the smaller ones may have an advantage for limited resources due to a higher rate of nutrient uptake at higher *T* (Peters 1983, Reuman et al. 2014).

Table 2. Coefficient of determination (r^2) and p-values for single-parameter models of phytoplankton sinking rate (Sr) constricted by the environmental variables of each season (summer and winter) as explanatory variables in Gouqi Island. *T*: temperature; S: salinity; DO: dissolved oxygen. The best models, selected based on Akaike's information criterion (AIC), are in **bold**

Season	No.	Single-parameter models	r^2	p	AIC
Summer	**1**	**Sr ~ 0.660 – 0.419 (NO_3^-)**	**0.594**	**<0.001**	**–72.69**
	2	Sr ~ 0.403 – 0.020 (NH_4^+)	0.126	0.031	–49.69
	3	Sr ~ 4.040 – 0.781 (DO)	0.020	0.216	–46.49
	4	Sr ~ 0.294 – 0.241 (NO_2^-)	0.019	0.462	–45.19
	5	Sr ~ –0.153 + 0.015 (*T*)	0.020	0.456	–45.14
	6	Sr ~ 0.210 + 0.002 (Depth)	0.024	0.410	–45.42
	7	Sr ~ 0.168 + 0.067 (PO_4^{3-})	0.023	0.419	–45.29
	8	Sr ~ 0.222 – 0.0001 (S)	0.000	0.971	–44.60
Winter	**1**	**Sr ~ –0.140 + 8.500 (NO3–)**	**0.345**	**<0.001**	**–67.97**
	2	Sr ~ 0.727 – 6.125 (NH_4^+)	0.281	0.002	–65.16
	3	Sr ~ 0.065 + 39.722 (NO_2^-)	0.014	0.244	–55.71
	4	Sr ~ 2.398 – 0.361 (DO)	0.000	0.324	–55.29
	5	Sr ~ –0.996 + 0.039 (S)	0.023	0.428	–54.92
	6	Sr ~ 0.210 – 0.001 (Depth)	0.021	0.445	–54.87
	7	Sr ~ –0.320 + 0.040 (*T*)	0.013	0.549	–54.62
	8	Sr ~ 0.173 + 0.223 (PO_4^{3-})	0.002	0.820	–54.29

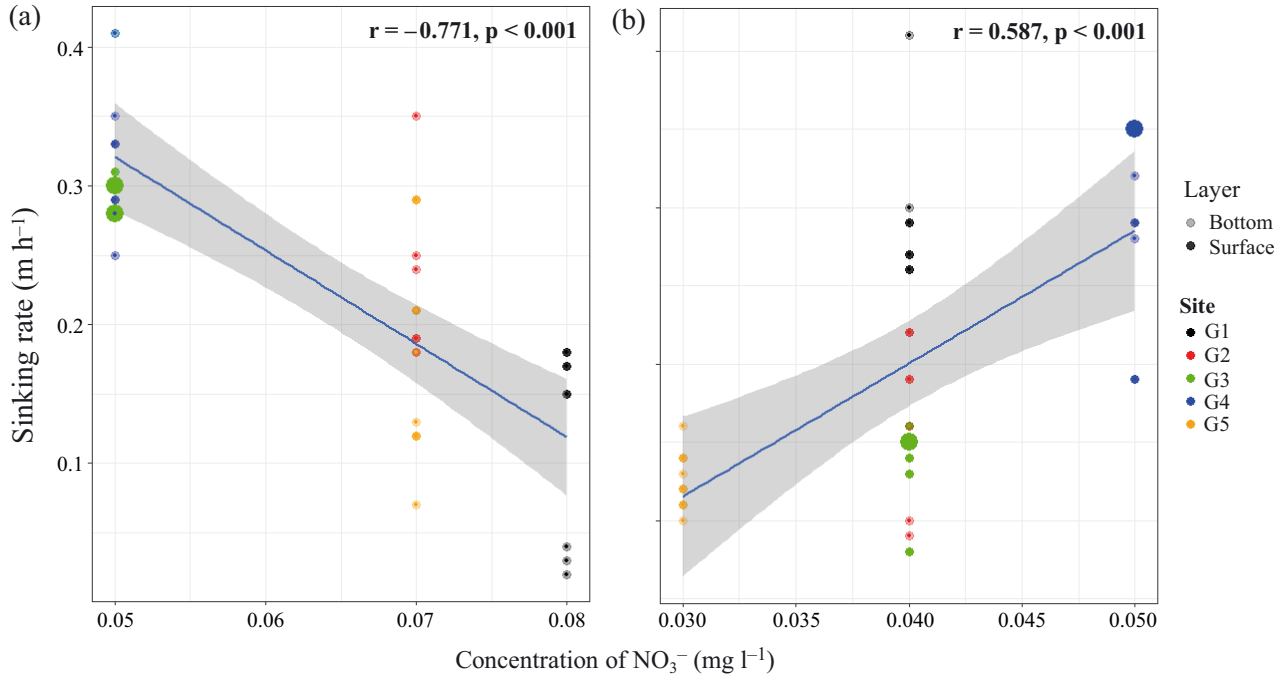

Fig. 7. Phytoplankton sinking rate fitted against the concentration of nitrate in (a) summer and (b) winter. Regression lines with a 95% confidence interval (shaded) and equations with the correlation coefficient are shown in each panel. Circle sizes represent numbers of the same value

Thus, the smaller-sized phytoplankton would be the dominant size class in winter.

In summer, NO_3^- and NH_4^+ were the main factors affecting the PSS. Compared with a coastal region near our study site in the East China Sea (Guo et al. 2016), the concentration of NO_3^- for both seasons in the study area was 10 times lower, while the concentration of NH_4^+ was relatively high. Such a low detectable concentration of NO_3^- should reduce phytoplankton photosynthetic capacity, growth, and biomass (Graziano et al. 1996). But the question remains why the chl *a* of large phytoplankton was still relatively high in Gouqi Island. One possibility is that the environmental nutrient concentration is primarily regulated by phytoplankton uptake (Torres-Valdés & Purdie 2006). In general, large phytoplankton with high biomass may selectively and strongly absorb NO_3^- (Domingues et al. 2011), thus resulting in low detectable concentrations. It should be noted that mussel aquaculture may also strongly affect these nutrient levels. A previous study showed that shellfish cultivation can enhance the removal of nutrients such as nitrogen from seawater through the process of biomass harvest (Taylor et al. 2019, Liu et al. 2021). This possibility suggests that mussel aquaculture is likely also responsible for the relatively low concentration of nitrogen. Meanwhile, the process of mussel feeding involves the consumption of phytoplankton and other suspended organic particles, sequestering organic carbon within their tissues and packaging waste into fecal pellets, thus enhancing the flux of organic carbon to the seafloor and potentially increasing carbon burial rates in sediments (Giles et al. 2006). The deposited organic matter in the sediment is predicted to be mineralized and induces the increase of NH_4^+ production due to dissimilatory NO_3^- reduction (Christensen et al. 2003, Carlsson et al. 2009, 2012, Nizzoli et al. 2011). Thus, intensive mussel aquaculture may strongly influence the NH_4^+ dynamics in Gouqi Island. To better understand the nutrient dynamics, future research is needed to explore nutrient cycling in the water column and sediments and assess their contribution to nutrient dynamics.

Among the nutrients, NO_3^- was negatively correlated with micro-sized phytoplankton, while NH_4^+ was positively associated with pico-sized phytoplankton. These results suggest that small phytoplankton possibly dominate under nitrogen-rich conditions (Site G1), whereas larger phytoplankton dominate under nitrogen-deficient conditions (Sites G2, G3, and G4) in our study area. However, this is contrary to previous findings about the relationship between PSSs and nutrient concentrations (Marañón et al. 2001, 2015, Maguer et al. 2009, Acevedo-Trejos et al. 2015, Marañón 2015, Mousing et al. 2018). The possible reason for this disparity is that the uptake preference for NH_4^+ and NO_3^- by phytoplankton is likely size-group-specific. In general, diatoms primarily utilize NO_3^-, while green algae and

cyanobacteria prefer NH_4^+ (Domingues et al. 2011). If this is the case, the positive relationships between pico-sized phytoplankton and NH_4^+ indicate that the small-size phytoplankton mainly consisted of green algae and cyanobacteria, while the negative association between NO_3^- concentration and the micro-sized group suggests that diatoms may contribute largely to the large phytoplankton. Accordingly, a previous study found that the dominant phytoplankton species in the farm boundary are large-sized diatoms (Chen & Zhang 2011, Guan et al. 2022). Given our study's lack of data on phytoplankton communities, further study is needed to substantiate our findings.

Moreover, NH_4^+ was found to be negatively related to nano-sized phytoplankton, suggesting that sites with high NH_4^+ levels may support less nano-sized phytoplankton. As mentioned earlier, smaller-sized phytoplankton may prefer NH_4^+ (Domingues et al. 2011). The occurrence of this phenomenon could be multifaceted. One possibility is the density-dependent selective feeding by mussels. The intensive farming of mussels might induce the production of NH_4^+, suggesting that sites with high NH_4^+ concentrations, such as Site G1, may indicate a relatively high cultivation density. Indeed, the offshore sites (G2, G3, and G5) experienced a reduction in cultivation density following harvest initiation in August. In contrast, the near-shore site (G1) maintained its farm density throughout the sampling period, possibly due to the relatively small size of mussels there, which were not yet harvested. Additionally, the intensive farming of mussels could lead to a strong removal rate of nano-sized phytoplankton (Li 2019, Zhang et al. 2024). Consequently, Site G1 exhibited a lower concentration of nano-sized phytoplankton.

In addition, we found that DO was positively correlated with pico-sized phytoplankton and negatively correlated with nano-sized phytoplankton in summer. This suggests a difference in oxygen production efficiency between the size classes during photosynthesis. A previous study documented that phytoplankton assemblages were dominated by smaller cells under warm conditions, having higher photosynthetic efficiencies (Robinson et al. 2018). Indeed, Site G1 exhibited a higher concentration of pico-sized phytoplankton compared to other sites, while also displaying higher DO levels in summer.

4.2. Effects of size structure on phytoplankton Sr

In this study, we examined the Sr by determining changes in total chl *a* concentration with the SETCOL method (Bienfang 1981, Pitcher et al. 1989). The results showed that the average Sr in summer was significantly higher than in winter. Stokes (1851) suggested that particle diameter could greatly and positively affect Srs. The differences in the size structure of the dominant phytoplankton groups between the 2 seasons were likely responsible for the variations in Srs. Moreover, we found that the Sr was positively related to the proportion of micro-sized phytoplankton in summer, while negatively related to the proportion of the smallest phytoplankton (0.2–2 µm) in both seasons. These results suggest that sites dominated by micro-sized phytoplankton may exhibit higher Srs in summer, while those dominated by pico-sized phytoplankton may display lower Srs in both seasons. Given the shift in size composition between seasons, some sites, such as G3, demonstrated higher Srs in summer and lower Srs in winter. This pattern suggests that the expression of Srs at these sites is likely regulated by the PSSs, as previously suggested by Takahashi & Bienfang (1983) and Mao et al. (2023).

It should be noted that the SETCOL-derived Sr based on chl *a* is thought to be consistently lower than that derived from cell counts (Pitcher et al. 1989). Moreover, the Sr measured by the SETCOL method is likely influenced by settling time. Although the settling time (2–3 h) used in this study may underestimate the Srs of some fast-sinking cells (>6.36 m d^{-1}) (Mao et al. 2023), the Sr measured in both seasons was far smaller than that. This suggests that the Sr was relatively reliable in this study.

4.3. Direct and indirect effects of environmental factors on phytoplankton Srs

As discussed above, the PSSs are responsible for the Srs, which are in turn greatly regulated by environmental factors. Our finding suggests that the environment may affect the Sr indirectly, as the key factors are different between seasons. In summer, NO_3^- was negatively related to micro-sized phytoplankton, while ammonia was positively related to pico-phytoplankton. Both of these size structures were also significantly associated with Sr, although the directions were opposite. The results suggest that nitrogen-related nutrients may play a role in affecting the Sr through PSS in summer. In winter, *T*, the most important environmental variable affecting the PSS, was positively related to smaller structures (2–20 µm), which was not correlated with Sr. This suggests that the measured environmental factors could not affect the Sr through PSS in winter.

We questioned whether there were any environmental factors affecting the Sr directly in winter. Interestingly, a positive correlation between Sr and NO_3^- was found, indicating that the Sr increases with increasing concentration of NO_3^-. However, this relationship is somewhat puzzling. In general, low nutrient levels often result in increased Srs because of a vertical migration strategy to acquire multiple resources from relatively deep layers (Muggli et al. 1996, Titman & Kilham 1976). This is also evidenced by our results in summer that Sr and NO_3^- were negatively related. It should be noted that Sr may also affect the material flux around algal cells via boundary layer replacement (Gavis 1976, Karp-Boss et al. 1996, Wolf-Gladrow & Riebesell 1997). A previous study found that nutrient flux in micro-sized phytoplankton increases during fast sinking and then increases their nutrient uptake from the ambient environment (Karp-Boss et al. 1996, Mann & Lazier 1996, Gemmell et al. 2016). Considering that the Sr was positively related to the micro-sized group in summer, the fast sinking of this dominant large phytoplankton may strongly remove the NO_3^- and thus result in a negative relationship between them.

However, the question remains as to why the opposite result occurs in winter. One possibility for this phenomenon is that faster-sinking phytoplankton may also promote the production of inorganic nitrogen (e.g. NO_3^-). In winter, the low *T* inhibits the biomass of large-size phytoplankton and may cause their death, thus inducing the production of phytoplankton-derived particulate organic matter by natural microbial communities (Wetz et al. 2008). This degradation rate of organic particles is likely accelerated by sinking (Alcolombri et al. 2021) and thus promotes the release of dissolved inorganic matter (Smith et al. 1992). This reasoning is supported by a previous study that an increase in NO_3^- concentrations in the open ocean has typically been directly connected with regions of increased sinking particles (Eppley & Peterson 1979). These possibilities suggest that faster-sinking organic matter not only contributes to the vertical flux of carbon but also promotes its own decomposition and thus produces inorganic matter.

5. CONCLUSIONS

This study examined the complex interactions between PSSs, Srs, and environmental factors within a high-density mussel farming environment. We found that the dominant size structures of phytoplankton were >20 and <20 µm in summer and winter, respectively, suggesting a dynamic shift in phytoplankton community composition. These dominant size groups were negatively related to NO_3^- in summer and positively related to *T* in winter, suggesting that NO_3^- and *T* may play roles in affecting the PSSs in summer and winter, respectively. Interestingly, in summer, the PSS including micro- and pico-sized phytoplankton could also strongly affect their Srs but in opposite directions, which are in turn mainly regulated by NO_3^-. This indicates that NO_3^- may affect the Sr indirectly via PSS in summer. Meanwhile, a direct effect of NO_3^- on Sr was also found in both seasons. However, the associations of the 2 variables were opposite between the 2 seasons, suggesting a complicated mutual interaction between Sr and nutrients. Therefore, Sr is not only regulated by NO_3^- but is also controlled by its feedback to changes in NO_3^- concentration.

Our results provide insights into the mechanisms driving phytoplankton export from the surface to the bottom water, particularly in the context of coastal waters where aquaculture activities are prevalent. Since our sampling period for each season is likely not sufficient to represent the seasonal dynamics, further studies with extended sampling durations or frequencies are necessary to confirm our findings. Moreover, considering the potential impact of mussel aquaculture on the phytoplankton community and carbon export, further study should also explore the role of mussel cultivation in regulating the biogeochemical processes within aquatic ecosystems.

Acknowledgements. This study was supported by the National Key Research and Development Program of China (2023YFD 2401903) and the Science and Technology Bureau of Zhoushan (2023C41004) to X.Z., and by the National Natural Science Foundation of China (32301320) and the Science and Technology Bureau of Zhoushan (2023C41018) to X.T.

LITERATURE CITED

Acevedo-Trejos E, Brandt G, Bruggeman J, Merico A (2015) Mechanisms shaping size structure and functional diversity of phytoplankton communities in the ocean. Sci Rep 5:8918

Agawin NSR, Duarte C, Agustí S (2000) Nutrient and temperature control of the contribution of picoplankton to phytoplankton biomass and production. Limnol Oceanogr 45:591–600

Alcolombri U, Peaudecerf FJ, Fernandez VI, Behrendt L, Lee KS, Stocker R (2021) Sinking enhances the degradation of organic particles by marine bacteria. Nat Geosci 14: 775–780

Atkinson D, Ciotti B, Montagnes D (2003) Protists decrease in size linearly with temperature: ca. 2.5% °C^{-1}. Proc R Soc B 270:2605–2611

Bienfang PK (1981) SETCOL — a technologically simple and reliable method for measuring phytoplankton sinking rates. Can J Fish Aquat Sci 38:1289–1294

Bienfang PK, Harrison PJ, Quarmby LM (1982) Sinking rate response to depletion of nitrate, phosphate and silicate in four marine diatoms. Mar Biol 67:295–302

Boyd PW, Trull TW (2007) Understanding the export of biogenic particles in oceanic waters: Is there consensus? Prog Oceanogr 72:276–312

Burnham KP, Anderson DR (2003) Model selection and multimodel inference: a practical information-theoretic approach. Springer Science & Business Media, New York, NY

Carlsson MC, Holmer M, Petersen JK (2009) Seasonal and spatial variations of benthic impacts of mussel longline farming in a eutrophic Danish Fjord, Limfjorden. J Sea Res 28:791–801

Carlsson MS, Engström P, Lindahl O, Ljungqvist L, Petersen JK, Svanberg L, Holmer M (2012) Effects of mussel farms on the benthic nitrogen cycle on the Swedish west coast. Aquacult Environ Interact 2:177–192

Cetinić I, Viličić D, Burić Z, Olujć G (2006) Phytoplankton seasonality in a highly stratified karstic estuary (Krka, Adriatic Sea). Hydrobiologia 555:31–40

Chen M, Zhang S (2011) The community structure of phytoplankton in Gouqi Island. Shanghai Haiyang Daxue Xuebao 20:607–612 (in Chinese with English Abstract)

Christensen PB, Glud RN, Dalsgaard T, Gillespie P (2003) Impacts of longline mussel farming on oxygen and nitrogen dynamics and biological communities of coastal sediments. Aquaculture 218:567–588

Deng M (2016) Effects of raft aquaculture on dynamics and phytoplankton ecosystem. MSc dissertation, Shanghai Ocean University (in Chinese with English Abstract)

Domingues RB, Barbosa AB, Sommer U, Galvão HM (2011) Ammonium, nitrate and phytoplankton interactions in a freshwater tidal estuarine zone: potential effects of cultural eutrophication. Aquat Sci 73:331–343

Eppley RW, Peterson BJ (1979) Particulate organic matter flux and planktonic new production in the deep ocean. Nature 282:677–680

Falkowski PG, Barber RT, Smetacek V (1998) Biogeochemical controls and feedbacks on ocean primary production. Science 281:200–207

Field CB, Behrenfeld MJ, Randerson JT, Falkowski P (1998) Primary production of the biosphere: integrating terrestrial and oceanic components. Science 281:237–240

Gavis J (1976) Munk and Riley revisited: nutrient diffusion transport and rates of phytoplankton growth. J Mar Res 34:161–179

Gemmell BJ, Oh G, Buskey EJ, Villareal TA (2016) Dynamic sinking behaviour in marine phytoplankton: rapid changes in buoyancy may aid in nutrient uptake. Proc R Soc B 283: 20161126

Graziano LM, Geider RJ, Li WKW, Olaizola M (1996) Nitrogen limitation of North Atlantic phytoplankton: analysis of physiological condition in nutrient enrichment experiments. Aquat Microb Ecol 11:53–64

Guan Y, Lin J, Jiao J, Liu H (2022) The characteristics of phytoplankton community of mussel raft farms and surrounding waters under high filtration pressure. Haiyang Huanjiang Kexue 41:543–553 (in Chinese with English Abstract)

Guidi L, Chaffron S, Bittner L, Eveillard D and others (2016) Plankton networks driving carbon export in the oligotrophic ocean. Nature 532:465–470

Guo S, Sun J, Zhao Q, Feng Y, Huang D, Liu S (2016) Sinking rates of phytoplankton in the Changjiang (Yangtze River) estuary: a comparative study between *Prorocentrum dentatum* and *Skeletonema dorhnii* bloom. J Mar Syst 154: 5–14

Iversen MH, Ploug H (2013) Temperature effects on carbon-specific respiration rate and sinking velocity of diatom aggregates — potential implications for deep ocean export processes. Biogeosciences 10:4073–4085

Jiang Y, He W, Liu W, Qin N and others (2014) The seasonal and spatial variations of phytoplankton community and their correlation with environmental factors in a large eutrophic Chinese lake (Lake Chaohu). Ecol Indic 40: 58–67

Jiang X, Li H, Tong S, Gao K (2022) Nitrogen limitation enhanced calcification and sinking rate in the coccolithophorid *Gephyrocapsa oceanica* along with its growth being reduced. Front Mar Sci 9:834358

Karp-Boss L, Boss E, Jumars P (1996) Nutrient fluxes to planktonic osmotrophs in the presence of fluid motion. Oceanogr Mar Biol Annu Rev 34:71–108

Kocum E (2020) Autotrophic nanoplankton dynamics is significant on the spatio-temporal variation of phytoplankton biomass size structure along a coastal trophic gradient. Reg Stud Mar Sci 33:100920

Lai J, Zou Y, Zhang J, Peres-Neto P (2022) Generalizing hierarchical and variation partitioning in multiple regression and canonical analyses using the rdacca.hp R package. Methods Ecol Evol 13:782–788

Li F (2019) Size fraction of phytoplankton and ecological contribution of microbial loop in large-scale bivalve mariculture area. MSc dissertation, Shanghai Ocean University, Shanghai (in Chinese with English Abstract)

Liu M, Wang Z, Zhang G (2021) Nitrogen removal through oyster cultivation: integration with artificial fertilization makes it more efficient. Sci Total Environ 792:148057

López-Urrutia Á, Morán XAG (2015) Temperature affects the size-structure of phytoplankton communities in the ocean. Limnol Oceanogr 60:733–738

Maguer JF, L'Helguen S, Waeles M, Morin P, Riso R, Caradec J (2009) Size-fractionated phytoplankton biomass and nitrogen uptake in response to high nutrient load in the North Biscay Bay in spring. Cont Shelf Res 29: 1103–1110

Mann KH, Lazier JRN (1996) Biology and boundary layers. In: Dynamics of marine ecosystems, 3rd edn. Blackwell Science, Cambridge, MA, p 7–67

Mao Y, Sun J, Guo C, Yang S, Wei Y (2023) Sinking rates of phytoplankton in response to cell size and carbon biomass: a case study in the northeastern South China Sea. J Mar Syst 240:103885

Marañón E (2015) Cell size as a key determinant of phytoplankton metabolism and community structure. Annu Rev Mater Sci 7:241–264

Marañón E, Holligan PM, Barciela R, González N, Mouriño B, Pazó MJ, Varela M (2001) Patterns of phytoplankton size structure and productivity in contrasting open-ocean environments. Mar Ecol Prog Ser 216:43–56

Marañón E, Cermeño P, Latasa M, Tadonléké RD (2012) Temperature, resources, and phytoplankton size structure in the ocean. Limnol Oceanogr 57:1266–1278

Marañón E, Cermeño P, Latasa M, Tadonléké RD (2015) Resource supply alone explains the variability of marine phytoplankton size structure. Limnol Oceanogr 60: 1848–1854

Mattei F, Buonocore E, Franzese PP, Scardi M (2021) Global assessment of marine phytoplankton primary production: integrating machine learning and environmental accounting models. Ecol Modell 451:109578

Mousing EA, Richardson K, Ellegaard M (2018) Global patterns in phytoplankton biomass and community size structure in relation to macronutrients in the open sea. Limnol Oceanogr 63:1298–1312

Muggli DL, Lecourt M, Harrison PJ (1996) Effects of iron and nitrogen source on the sinking rate, physiology and metal composition of an oceanic diatom from the subarctic Pacific. Mar Ecol Prog Ser 132:215–227

Naselliflores L (2000) Phytoplankton assemblages in twenty-one Sicilian reservoirs: relationships between species composition and environmental factors. Hydrobiologia 424:1–11

Nizzoli D, Welsh DT, Viaroli P (2011) Seasonal nitrogen and phosphorus dynamics during benthic clam and suspended mussel cultivation. Mar Pollut Bull 62:1276–1287

Peters RH (1983) The ecological implications of body size. Cambridge University Press, Cambridge

Pitcher GC, Walker DR, Mitchell-Innes BA (1989) Phytoplankton sinking rate dynamics in the southern Benguela upwelling system. Mar Ecol Prog Ser 55:261–269

Pulina S, Satta CT, Padedda BM, Sechi N, Lugliè A (2018) Seasonal variations of phytoplankton size structure in relation to environmental variables in three Mediterranean shallow coastal lagoons. Estuar Coast Shelf Sci 212: 95–104

Qu L, Thomas LN, Wienkers AF, Hetland RD and others (2022) Rapid vertical exchange at fronts in the Northern Gulf of Mexico. Nat Commun 13:5624

R Core Team (2019) R: a language and environment for statistical computing. R Foundation for Statistical Computing, Vienna

Radchenko IG, Il'yash LV (2006) Growth and photosynthetic activity of diatom *Thalassiosira weissflogii* at decreasing salinity. Biology Bull 33:242–247

Reuman DC, Holt RD, Yvon-Durocher G (2014) A metabolic perspective on competition and body size reductions with warming. J Anim Ecol 83:59–69

Robinson A, Bouman HA, Tilstone GH, Sathyendranath S (2018) High photosynthetic rates associated with pico and nanophytoplankton communities and high stratification index in the North West Atlantic. Cont Shelf Res 171: 126–139

Shiomoto A, Inoue K (2020) Seasonal variations of size-fractionated chlorophyll *a* and primary production in the coastal area of Hokkaido in the Okhotsk Sea. SN Appl Sci 2:1880

Sieburth JM, Smetacek V, Lenz J (1978) Pelagic ecosystem structure: heterotrophic compartments of the plankton and their relationship to plankton size fractions. Limnol Oceanogr 23:1256–1263

Silver MW, Shanks AL, Trent JD (1978) Marine snow: microplankton habitat and source of small-scale patchiness in pelagic populations. Science 201:371–373

Smayda TJ (1970) The suspension and sinking of phytoplankton in the sea. Oceanogr Mar Biol Annu Rev 8:353–414

Smith VH (1982) The nitrogen and phosphorus dependence of algal biomass in lakes: an empirical and theoretical analysis. Limnol Oceanogr 27:1101–1112

Smith DC, Simon M, Alldredge AL, Azam F (1992) Intense hydrolytic enzyme activity on marine aggregates and implications for rapid particle dissolution. Nature 359: 139–142

Stokes GG (1851) On the effect of internal friction of fluids on the motion of pendulums. Trans Camb Phil Soc 9:8–14

Takahashi M, Bienfang PK (1983) Size structure of phytoplankton biomass and photosynthesis in subtropical Hawaiian waters. Mar Biol 76:203–211

Taylor D, Saurel C, Nielsen P, Petersen JK (2019) Production characteristics and optimization of mitigation mussel culture. Front Mar Sci 6:698

Tian C, Pei H, Hu W, Xie J (2013) Phytoplankton variation and its relationship with the environmental factors in Nansi Lake, China. Environ Monit Assess 185:295–310

Titman D, Kilham P (1976) Sinking in freshwater phytoplankton: some ecological implications of cell nutrient status and physical mixing processes. Limnol Oceanogr 21:409–417

Torres-Valdés S, Purdie DA (2006) Nitrogen removal by phytoplankton uptake through a temperate non-turbid estuary. Estuar Coast Shelf Sci 70:473–486

van Ierland ET, Peperzak L (1984) Separation of marine seston and density determination of marine diatoms by density gradient determination. J Plankton Res 6:29–44

Waite AM, Fisher A, Thompson PA, Harrison PJ (1997) Sinking rate versus cell volume relationship illuminate sinking rate control mechanisms in marine diatoms. Mar Ecol Prog Ser 157:97–108

Wang L, Wang C, Deng D, Zhao X, Zhou Z (2015) Temporal and spatial variations in phytoplankton: correlations with environmental factors in Shengjin Lake, China. Environ Sci Pollut Res Int 22:14144–14156

Welschmeyer NA (1994) Fluorometric analysis of chlorophyll-*a* in the presence of chlorophyll-*b* and pheopigments. Limnol Oceanogr 39:1985–1992

Wetz MS, Hales B, Wheeler PA (2008) Degradation of phytoplankton-derived organic matter: implications for carbon and nitrogen biogeochemistry in coastal ecosystems. Estuar Coast Shelf Sci 77:422–432

Wolf-Gladrow D, Riebesell U (1997) Diffusion and reactions in the vicinity of plankton: a refined model for inorganic carbon transport. Mar Chem 59:17–34

Yang EJ, Choi JK, Hyun J (2008) Seasonal variation in the community and size structure of nano- and microzooplankton in Gyeonggi Bay, Yellow Sea. Estuar Coast Shelf Sci 77:320–330

Yin D, Zheng L, Song L (2011) Spatio-temporal distribution of phytoplankton in the Danjiangkou Reservoir, a water source area for the South-to-North Water Diversion Project (Middle Route), China. Chin J Oceanology Limnol 29:531–554

Zhang S, Wang L, Wang W (2008) Algal communities at Gouqi Island in the Zhoushan archipelago, China. J Appl Phycol 20:853–861

Zhang R, Fang J, Zhang Y, Qin X, Zheng X, Zeng C, Wang J (2024) Effects of mussel–phytoplankton interactions on the aquatic environment. Aquacult Rep 37:102242

Editorial responsibility: Antonio Bode, A Coruña, Spain
Reviewed by: 3 anonymous referees

Submitted: May 25, 2024
Accepted: September 5, 2024
Proofs received from author(s): October 12, 2024